



Design of a Multiple Exploding Wire Setup to Study Shock Wave Dynamics

W. Mellor¹ · E. Lakhani¹ · J.C. Valenzuela² · B. Lawlor² · J. Zantesson¹ · V. Eliasson¹ 

Received: 26 September 2018 / Accepted: 1 October 2019 / Published online: 5 November 2019
© The Society for Experimental Mechanics, Inc 2019

Abstract

Shock wave dynamics is a topic with a wide variety of applications ranging from removal of kidney stones to inertial confinement fusion. In reality, the shock front is most often followed by a decay in flow properties, and therefore it is of interest to better understand shock dynamic events for these situations. Thus, an experimental facility that can provide results that are accurate, highly controlled, affordable and with a quick turn-around time are needed. Here, we present the design of an exploding wire system that can be coupled to either a two-dimensional or a three-dimensional test section to provide the user with a multitude of settings to study shock dynamics emanating from shock waves with decaying flow properties behind the shock front. Schlieren photographs taken with an ultra-high speed camera are also presented to show that the exploding wire system functions as intended in both two- and three-dimensional setups.

Keywords Exploding wire · Shock wave dynamics · Schlieren · High-voltage

Introduction

Shock wave dynamics is an area of research where applications may span from the medical field [1] to fusion ignition techniques [2]. Shock wave dynamics can be studied experimentally using different types of techniques, and the most common one is through the use of shock tubes. Oftentimes, shock tubes feature constant cross section area geometries such that the flow properties behind the shock front remain constant for an extended period of time [3]. Moreover, many shock tube experiments are two-dimensional by nature of the shock tube setup, see e.g. [4, 5], and thus three-dimensional experimental results (at least in open literature) are rather scarce. Thus, if one wishes to

study shock dynamics where the flow properties behind the shock front resembles that of a blast wave (with decaying flow properties behind the shock front) an exploding wire setup may be the answer – provided it is safe to use and can deliver repeatable results.

Exploding wire systems are not novel setups in the realm of experimentation [6], but have actually been used since 1773 [7, 8]. These setups were used for many different types of research areas, such as Ernst Mach's study of shock reflections in the 1870s [9], studies of thin metal films [10], and spectral studies [11–13]. Not until 1959 [14] came the first schlieren visualizations of shock waves that were generated by exploding wires. However, the use of exploding wires for the study of shock wave dynamics was largely unexplored until the early 1990s [15]. Shock wave focusing experiments in a gaseous environment using exploding wires were performed in the early 2000s by Apazidis et al [16]. Perhaps more common has been the use of exploding wires in liquid environments, mainly with the purpose of studying high-energy density physics phenomena [17]. In these studies, underwater shock focusing was successfully generated by an array of exploding wires [18–22]. The drawback from this type of setup is its somewhat limited physical size, with an initial converging shock radius of about 10 mm – leading to extreme demands on both spatial and temporal resolution on any imaging devices used to visualize the shock dynamics events.

This study was partially supported by the US Air Force Research Laboratory under grant No. FA8651-17-1-004 and the National Science Foundation under grant number CBET-1803592.

✉ V. Eliasson
eliasson@ucsd.edu

¹ Department of Structural Engineering,
University of California San Diego, La Jolla,
CA 92093-0085, USA

² Department of Mechanical and Aerospace Engineering,
University of California San Diego, La Jolla,
CA 92093-0411, USA

Our goal with this exploding wire setup (EWS) was to create a versatile but robust and highly repeatable tool to allow for the study of shock wave dynamics in two or three dimensions. Therefore, care was taken to design the different blast chamber setups to allow the user as much freedom and variability as needed. Herein, a description of such an exploding wire setup is given in detail with results to show that it functions as expected.

Experimental Setup

The experimental setup consists of a driver unit, a test section and a visualization system. In the following sections all of the components of the exploding wire system will be described in detail to aid with the full understanding of the experimental technique. However, it should be noted that the novelty in this setup lies in the driver unit and its coupling with a two or three-dimensional test section of choice. In particular, one major design goal was to leave the ability to handle future experimental needs not known today to be interchanged with the driver unit as a whole,

allowing for modular system that can readily be extrapolated upon [23].

Driver Unit

The driver unit of the EWS is comprised of four main parts: a charging circuit; a load circuit; a damping circuit; and a triggering mechanism. The driver unit was constructed on top of a cart built of aluminum plates with wheels attached to it so that the setup can be moved around easily in the laboratory. The outer frame of the driver unit is created using aluminum struts and aluminum sheets to allow the cart to be grounded and work as a Faraday cage. This terminal is always connected to ground as is seen in the circuit diagram in Figure 1. Precaution due to the high-voltage application was taken in the design choice of the cart materials, part spacing, and rounding of sharp edges. The underlying purpose in all of these considerations was to reach a maximum charging voltage of 40 kV. By ensuring that all cart superstructure materials are conducting, in the case that any accidental discharge were to occur, it could safely be lead to a ground.

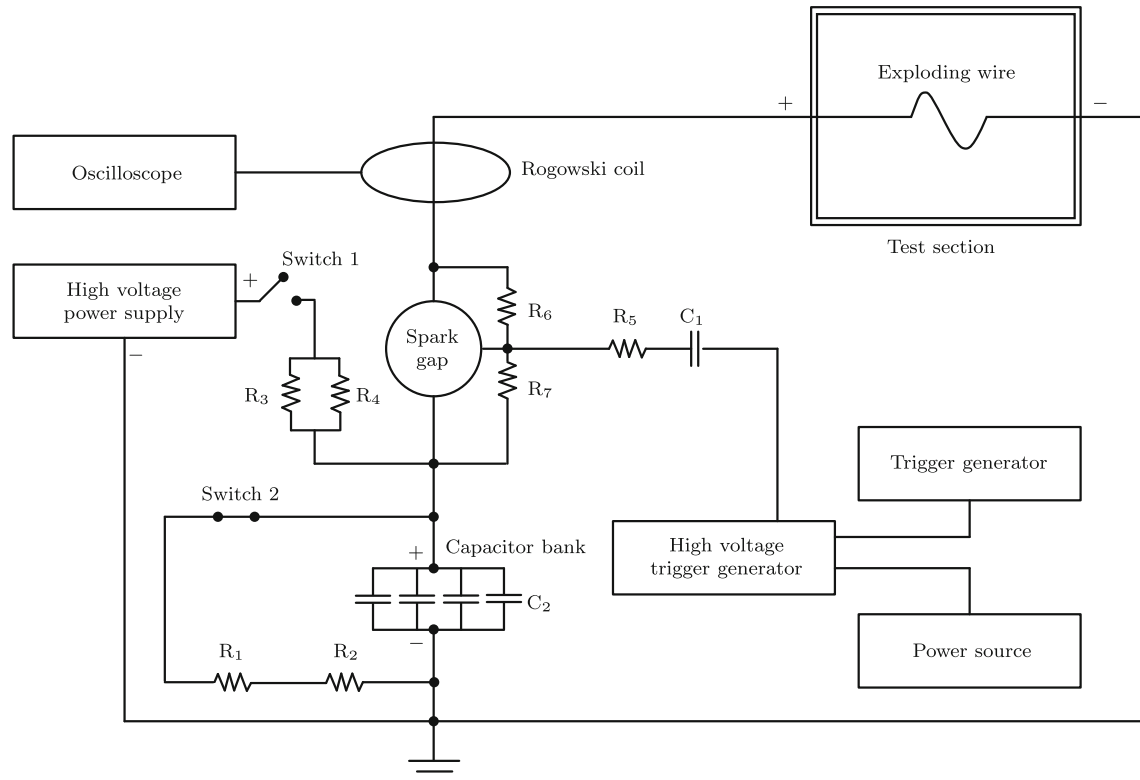


Fig. 1 Circuit diagram of the exploding wire system

Charging circuit

The charging circuit consists of four main parts: (1) a capacitor bank, (2) a high-voltage power supply, (3) a switch and (4) resistors.

The capacitor bank consists of four capacitors (0.22 μ F, General Atomics, Part No. 31160) connected in parallel. The capacitors are charged using a DC high-voltage source (50 kV, Glassman High Voltage Inc., Model No. FJ50N2.4). The capacitors are placed such that their positive terminals are facing inwards (towards each other) so that they can all be connected easily to one another. The negative terminals of these capacitors are connected to ground.

The switch, annotated as 'Switch 1' in Fig. 1, is a two-way switch (Ross Engineering, Model No. E40-DT-60). This is a *normally open* switch meaning that unless external power is supplied to the switch, it remains in the off position. The reason for having a normally open switch is to ensure that when the experiment is not running, the charging circuit remains open and the capacitors remain uncharged.

The resistors, annotated as R_3 and R_4 in Fig. 1, are 10 $M\Omega$ each (Vishay Dale Electronics Inc., Part No. BFW10M0LF08) and connected in parallel and they limit the charging current.

The charging unit works as follows: the high-voltage supply is connected to a regular wall socket and when Switch 1 is engaged current can flow through the circuit and charge the capacitors to the desired voltage. When designing the charging circuit, each component was chosen such that it was rated for a maximum voltage and power greater than the respective voltage and power that the component is expected to encounter during the experiment.

Damping circuit

The damping circuit consists of three main parts: (1) the same capacitor bank as in the charging circuit, (2) a switch, and (3) resistors.

The switch in this circuit, annotated 'Switch 2' in Fig. 1, is the same type of two-way switch as used in the charging circuit. However, this switch is a *normally closed* switch, which means that it remains in a closed position unless external power is supplied to it. This ensures that when the experiment is not running both the terminals of the capacitors are grounded for the safety of anyone using the space around the experimental setup.

The resistors, annotated R_1 and R_2 (1 $k\Omega$, Pulse Power and Measurement (PPM) Ltd., Series 508AS), are connected in series and they facilitate a quick capacitor discharge, within the components limitations.

Load circuit

The load circuit consists of the capacitor bank (described previously), a spark gap switch and exploding wires placed inside the test section. The spark gap switch essentially acts like a *normally open* switch. It only allows conduction in one of the two following instances: either when a high voltage trigger pulse is sent to it, or when the pressure inside the spark gap switch is lowered beyond the self-breakdown level. In either instance, once the spark gap reaches the self-breakdown level, the entirety of the charge in the capacitor bank is sent cascading forward into the wires going into the test section.

The connections from the spark gap switch (10-65 kV, Hofstra Group, Item No. 3114) to the exploding wires were made using a flexible coaxial cable (Pasternack Enterprises Inc.). A coaxial cable has two conductors separated by an insulator. Here, the inner conductor connects to the spark gap switch and the outer mesh connects to the ground (or negative) terminal of the capacitor bank. When the spark gap switch allows flow of current through it, the inner conductor will be connected to the positive terminal of the capacitor bank. The two ends of the exploding wires are then attached to the two conductors in the coaxial cable to complete the circuit. Also, the use of the coaxial cables is critical for timing for this experimental setup: due to the cable propagation delay (depending on the cable length) the user can apply the same voltage for an extended period of time to all the wires and thus ensuring that all wires explode at the same time.

Finally, a Rogowski coil (Pearson Electronics) connected to the positive side of the exploding wire was used to monitor the changing current. It also provided the synchronization signal to trigger the high-speed camera

Triggering mechanisms

The EWS has two main options in terms of triggering mechanisms: electrically or pneumatically. Depending upon the application, the user has to decide which one is most beneficial to add to the setup. The only main difference (besides cost) is that the electrically triggered configuration allows for a more precise discharge timing compared to the pneumatic case. But, in this presented study, the timing is not critical because the high-speed camera can be triggered off the current signal.

For some of the results presented here, an external electrical high-voltage trigger generator (model PT-55, Pacific Atlantic Electronics) was used. The PT-55 was powered up to 5 kV by a DC power supply (Glassman High Voltage Inc. Model No. FJ10P12, 10 kV), and it was subsequently triggered by a separate trigger generator that

produced a trigger pulse of 300 V amplitude, 200 ns width, and a maximum 10 ns rise time that was developed by the High Energy Density Physics Group at University of California San Diego [24]. Following the recommendations provided by the manufacturer of the spark gap switch, additional components were used to ensure its correct operation: a $150\ \Omega$ resistor annotated R_5 in Fig. 1 (Ohmite), two $100\ M\Omega$ resistors annotated R_6 and R_7 (Ohmite), and a $850\ pF$ capacitor annotated C_1 (TDK Corporation).

If the application does not need an electrical trigger unit, it could be beneficial to explore a pneumatic trigger. For the current setup the efficiency of triggering via pressure regulation is higher than when using an electrical impulse. In order to trigger electrically when running the EWS system at its maximum capacity, 40 kV in this case, a pressure control system would inevitably be needed to prevent any accidental breakdown of the system, and thus an unintentional firing. Without the pressure regulation, the system could be dangerous to operate, and inconsistent in terms of experimental parameters. Alternatively, when the system is triggered via a pneumatic operation by simply pressurizing above the self-breakdown limits of the spark gap, and then through an evacuation of pressure upon reaching the desired charging capacity. Upon the evacuation of pressure, the spark gap would then reach the zone of self-breakdown and effectively fire. Here, by omitting the PT-55, and thus the external trigger and high-voltage power supply, the required parts to operate the EWS decreased, and therefore reducing costs and space required for the EWS, minimizing potential hazards, and removing unnecessary operational steps that lead to a quicker experimental turn-around time. In this case, the pneumatic triggering of the spark gap relied on a pressure control box, Fig. 2.

The pressure control box regulated the incoming compressed air to the spark gap. A pressure evacuation line from the spark gap was then connected to three-way direct

action solenoid valve and subsequently a trigger in order to induce firing. Pneumatic triggering may be more efficient when utilizing capacitances greater than 25 kV, however, at capacitances lower than this, sub-atmospheric pressure is required in order to induce a breakdown of the spark gap. This can be achieved through the use of a vacuum pump coupled to the end of the evacuation line.

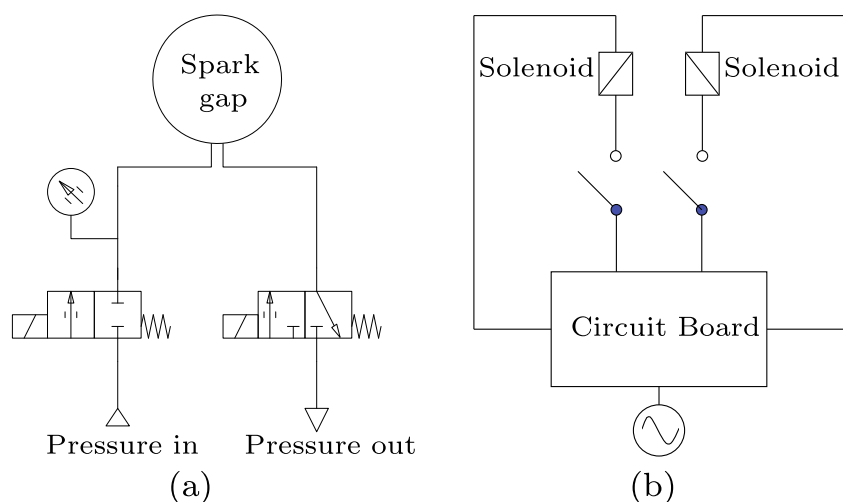
Test Sections

Here, two test sections are introduced; a two-dimensional test section to study cylindrical shocks and a three-dimensional test section to study spherical shocks. It should be noted that design emphasis was taken in allowing for a platform in which future experimental modules could be built upon. The initial designs chosen are meant to better visualize and capture particular shock-shock interactions, specifically, regular to irregular transitions, as well as three-dimensional shock expansion. Configurations of any design may be implemented depending on future needs.

Two-dimensional test section

The two-dimensional test section is a rectangular box with inner dimensions 500 mm (20 in) high, 500 mm (20 in) width and 19 mm (0.75 in) depth as shown in Fig. 3. The side windows are made out of 6.35 mm (0.25 in) thick transparent Polymethyl methacrylate (PMMA) sheets to allow for high-speed schlieren visualization of the shock waves. The exploding wires are located in between the 19 mm-space between the two windows. Each exploding wire is held in place using two circular brass electrodes containing a v-shaped notch, Fig. 3. The exploding wires rest on these electrodes. Small 10 g weights were attached at the two ends of the exploding wires to allow the wires to remain taut during the course of the experiment. The

Fig. 2 Schematic of the pressure control box. **a** Pneumatic lines and direct acting valves that control the pressure inside the spark gap. **b** Electrical circuit used to control the direct acting solenoid valves. The three-way valve connected to the evacuation line serves as the manual trigger to induce an electrical breakdown of the spark gap, and thus firing of the exploding wire system



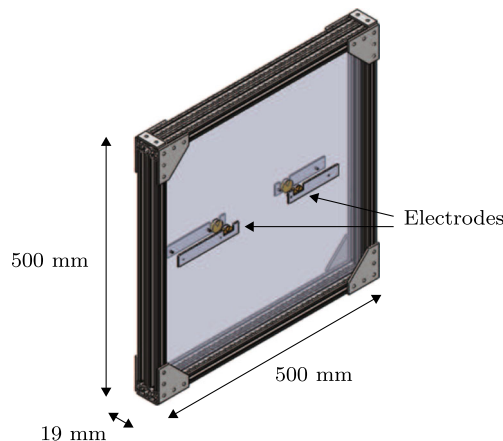


Fig. 3 Model of the two-dimensional test section with PMMA windows (inner test section dimension). The inside gap in between the two PMMA windows is 19 mm. Each exploding wire is held in place using two circular brass electrodes with a v-shaped notch

two brass electrodes used for each wire, located inside each PMMA window, are connected to the two opposite terminals of the capacitors using the coaxial cable, thereby completing the EWS circuit. All other connections in the circuit are designed for high-voltage levels except the exploding wires, thus ensuring that the explosion will occur inside the blast chamber. After the explosion, since the space between the two PMMA windows is small, the shock waves are constrained to propagate in a two-dimensional space only, leading to a two-dimensional shock wave being generated, i.e. a cylindrically outward propagating shock surface.

The number and locations of the exploding wires can easily be changed by varying the pattern of holes in the PMMA windows without adding significant cost to the setup.

Three-dimensional test section

The three-dimensional test section is a rectangular box that is 568 mm (22.4 in) high, 625 mm (24.6 in) width and 527 mm (20.8 in) depth shown in Fig. 4. All of test section windows are made out of 6.35 mm (0.25 in) thick transparent polycarbonate paneling. Additionally, the exploding wires and method of detonation is the same as the two-dimensional setup. However, unique to this construction is the use of a tower design to support the wires inside the chamber, as shown in Fig. 5. A tower is here defined as the setup required to ignite a wire. A single tower installment consists of one v-shaped notched brass electrode placed atop a variably tall optical post. To complete the wire setup, two of these towers are placed some distance apart from one another and the wire is strung across the brass electrodes. Again, the wire is held taut

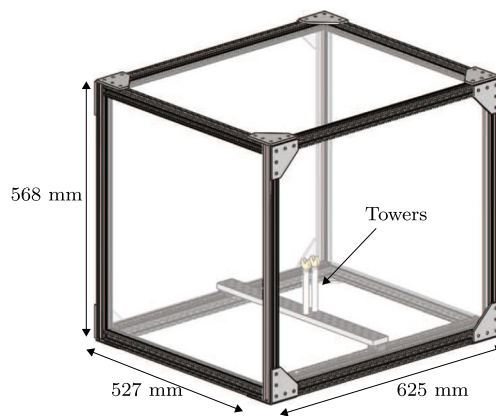


Fig. 4 Model of the three-dimensional test section with polycarbonate windows. Each exploding wire is held using two tower structures that are equipped with circular brass electrodes that contain a v-shaped notch at the top of the tower

by the addition of a small 10 g weights at the ends. Each brass electrode is separated electrically from one another with a non-conducting material to ensure that no accidental short-circuiting occurs when discharging the capacitor bank. Additionally, mounted to the top of the towers is a steel conducting plate where high-voltage coaxial cables connect the tower to the capacitor system. When multiple shock interactions are of interest, multiple towers can be mounted independently of one another. This allows for the strength of the shock waves, as well as geometric configurations, to be fully tunable.

Visualization System

All experimental results were obtained through the utilization of a z-folded schlieren system. All associated equipment is mounted upon optical breadboards placed on either side of the EWS test section. A careful description of a similar z-folded schlieren system can be found in our previous

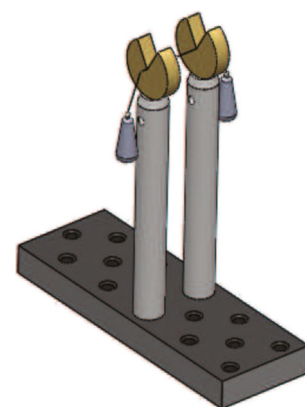
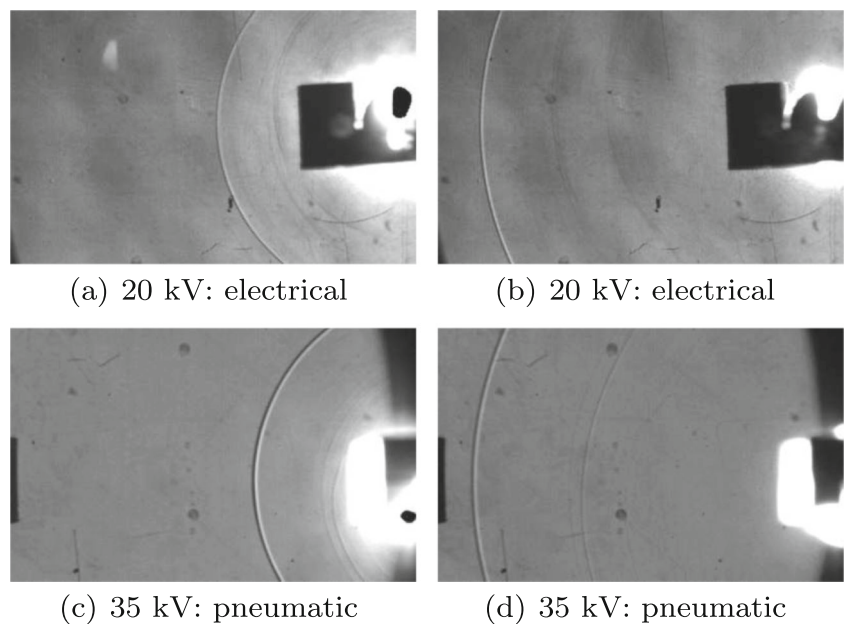


Fig. 5 Model of the tower systems used to support an exploding wire in the three-dimensional setup

Fig. 6 Schlieren photographs at an early (left column) and late (right column) time instant taken during an experiment in the two-dimensional test section. The shock wave is propagating from the right to the left. Photographs in (a) and (b) are taken with the electrical PT-55 trigger using 20 kV, while (c) and (d) are taken using the pneumatic trigger setup using 35 kV. The resolution is 400×250 pixels and the viewing area is approximately $130 \times 80 \text{ mm}^2$



work [25]. Either a light emitting diode or a pulsed laser diode is utilized as a point light source, which is subsequently passed through a series of mirrors placed in a z-type orientation. Passing first off a single concave mirror, light is collimated and turned through the test section by a flat mirror. Afterwards, the collimating process is reversed, and the light is redirected back into a point source where a schlieren knife edge is placed. Specifically for the photographs shown here, a knife edge in the shape of a pinhead 2 mm in diameter was used to create the schlieren effects observed in all radial flow directions. The size and position of the knife edge along with focusing mirrors was selected by means of trial and error in order to reduce both the interference from the initial explosion, and retain visual focus of the desired area of the test section.

Results

In order to validate both the effectiveness and the versatility of the proposed setup, here we present several

experimentally obtained results. Utilizing both the two-dimensional and three-dimensional test sections, shock interactions – in which the shock waves have decaying properties behind the shock front – obtained from this exploding wire system can be analyzed. Furthermore, given the provided experimental freedom with changeable parameters such as peak voltage, wire diameter and geometric location of the individual wires, observations can be tuned to specifically focus upon any phenomena of interest. Additionally, all of this can be done with a quick experimental turn-around time on the order of minutes.

Single expanding cylindrical shock

Figure 6 shows four images from a sequence of an expanding shock wave in the two-dimensional test section of which (a) and (b) are obtained using electrical triggering and (c) and (d) are obtained using pneumatic triggering. Utilizing the two-dimensional test section and a 0.05-mm diameter nickel chromium wire with a load current of

Fig. 7 Schlieren photographs taken during an experiment in the three-dimensional test section where two exploding wires are exploded at the same time. The resulting shock waves are propagating from the bottom to the top with the intersection point in the middle of the photograph. The resolution is 400×250 pixels and the viewing area is approximately $130 \times 80 \text{ mm}^2$

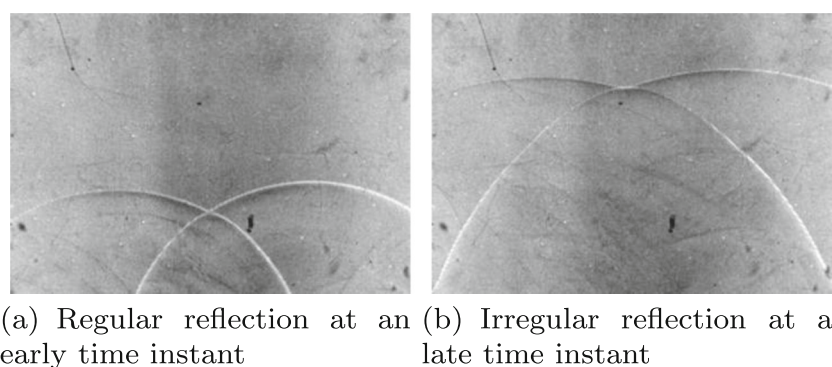
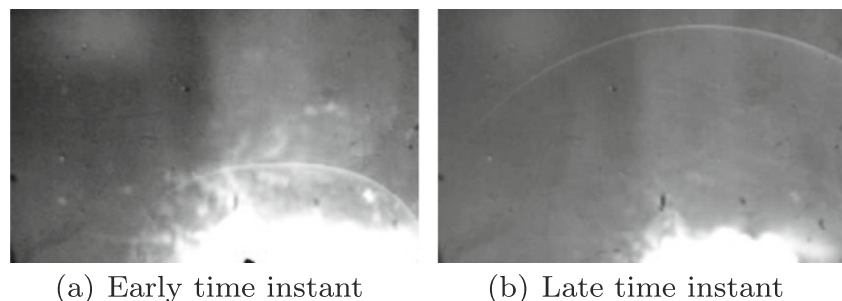


Fig. 8 Schlieren photographs taken during an experiment in the three-dimensional test section to measure how fast an ellipsoidal shock front becomes spherical. The resolution is 400×250 pixels and the viewing area is approximately $130 \times 80 \text{ mm}^2$



20 kV, the resulting images are photographs taken at a corresponding frame rate of 500,000 frames per second. Combining visual schlieren techniques alongside the experimental setup, allows insight into the deeper analysis of shock-shock interaction, Mach stem formation, and obstacle interaction. Coupling of the acquired experimental videos alongside e.g. Matlab codes yields analytical information that can be used to further interpret results quantitatively.

Regular to irregular transition for cylindrical shocks

Two photographs from a three-dimensional experiment are shown in Fig. 7. Two 0.05-mm-diameter nickel chromium wires were exploded at a capacitor charge voltage of 20 kV. The wires were spaced 76 mm (3 in) from one another and the resulting shock wave interaction was observed. The photographs in Fig. 7 are taken at a frame rate of 500,000 frames per second. This experiment validates the ability of the EWS to visualize the regular (two-shock system) to irregular (three-shock system) interaction of two three-dimensional shock waves in a very straight forward manner.

Evolution from ellipsoidal to spherical shock

The evolution of an ellipsoidal expanding shock wave towards a spherical expanding shock wave could be of interest as well, see Fig. 8. It can be observed that in the early time state after explosion, that the shock wave starts propagating as an ellipsoid. In a later time instant the shock wave has nearly transitioned into a spherical shock front. From this setup, the time and speed with which this transition occurs can be analyzed.

Conclusion

A novel experimental setup has been presented and shown to be effective in terms of better visualizing and studying shock waves with decaying flow properties behind the shock front. Experimental parameters, in regards to the

shock waves generated are fully tunable and can easily be adapted to work in concert with schlieren optical systems. Through meticulous system design, a fully modular and customizable exploding wire system platform has been created that is capable of meeting present as well as future experimental needs in order to quantitatively and qualitatively examine shock-shock interactions and other shock dynamics phenomena.

Acknowledgements This study was partially supported by the US Air Force Research Laboratory under grant No. FA8651-17-1-004 and the National Science Foundation under grant number CBET-1803592. VE wants to thank Mr. J. Gross, Mr. F. Zignum and Dr. A. Kuthi for help with the first exploding wire setup that lead to this one.

Compliance with Ethical Standards

Conflict of interests All authors state that there are no conflicts of interest.

References

1. Lingeman J, Kim S, Kuo R, McAteer J, Evan A (2003) Shockwave lithotripsy: Anecdotes and insights. *J Endourol* 17(9):687–693
2. Lindl J, Landen O, Edwards J, Moses E (2014) NIC Team: Review of the national ignition campaign 2009–2012. *Phys Plasmas* 21:014501
3. Anderson JJ (1990) Modern compressible flow: With historical perspective. McGraw-Hill, New York
4. Eliasson V, Apazidis N, Tillmark N (2007) Controlling the form of strong converging shocks by means of disturbances. *Shock Waves* 17:29–42
5. Eliasson V, Tillmark N, Szeri AJ, Apazidis N (2007) Light emission during shock wave focusing in air and argon. *Phys Fluids* 19:106106
6. Apazidis N, Eliasson V (2019) Shock focusing phenomena. Springer International Publishing
7. McGrath J (1966) Exploding wire research 1774–1963. Technical report, NRL Memorandum Report 1698, US Naval Research Laboratory
8. Nairne E (1774) VII. Electrical experiments by Mr. Edward Nairne, of London, mathematical instrument-maker, made with a machine of his own workmanship, a description of which is prefixed. *Phil Trans* 64:79–89
9. Blackmore J (1972) Ernst Mach; his work, life, and influence. University of California Press, Los Angeles
10. Toepler M (1898) Beobachtung von metalldampfschichtung bei elektrischer drahtzerstäubung. *Ann Phys* 65:873–876

11. Anderson J (1920) The spectrum of electrically exploded wires. *Astrophys J* 51:37–48
12. Anderson J (1922) The spectral energy distribution and opacity of wire explosion vapors. In: *Proceedings of the National Academy of Sciences of the United States of America*, vol 8, pp 231–232
13. Anderson J (1934) Electrically exploded wires. In: *International Critical Tables*. McGraw-Hill, New York
14. Sakurai A (1959) Chapter: on the propagation of cylindrical shock waves. In: *Exploding wires*. Plenum Press, New York
15. Higashino F, Henderson L, Shimizu F (1991) Experiments on the interaction of a pair of cylindrical weak blast waves in air. *Shock Waves* 1(4):275–284
16. Apazidis N, Lesser M, Tillmark N, Johansson B (2002) An experimental and theoretical study of converging polygonal shock waves. *Shock Waves* 12:39–58
17. Fedotov A, Grinenko A, Efimov S, Krasik Y (2007) Generation of cylindrically symmetric converging shock waves by underwater electrical explosion of wire array. *Appl Phys Lett* 90(20):201502–3
18. Efimov S, Fedotov A, Gleizer S, Gurovich V, Bazalitski G, Krasik Y (2008) Characterization of converging shock waves generated by underwater electrical wire array explosion. *Physics of Plasmas* 15:112703–5
19. Gilburd L, Efimov S, Fedotov Gefen A, Gurovich V, Bazalitski G, Antonov O, Krasik Y (2012) Modified wire array underwater electrical explosion. *Laser Particle Beams* 30(02):215–224
20. Krasik Y, Fedotov A, Sheftman D, Efimov S, Sayapin A, Gurovich V, Veksler D, Bazalitski G, Gleizer S, Grinenko A, Oreshkin V (2010) Underwater electrical wire explosion. *Plasma Sour Sci Technol* 19(3):034020–9
21. Krasik Y, Grinenko A, Sayapin A, Efimov S, Fedotov A, Gurovich V, Oreshkin V (2008) Underwater electrical wire explosion and its applications. *IEEE Trans Plasma Sci* 36(2):423–434
22. Veksler D, Sayapin A, Efimov S, Krasik Y (2008) Characterization of different wire configurations in underwater electrical explosion. *IEEE Trans Plasma Sci* 37(1):88–98
23. Lakhani E (2018) Design of exploding wire system. Master's thesis, University of California San Diego
24. Beg F High Energy Density Physics Group at UC San Diego. <http://fbeg.ucsd.edu/>
25. Wang C, Eliasson V (2012) Shock wave focusing in water inside convergent structures. *Int J Multiphys* 6:267–282

Publisher's Note Springer Nature remains neutral with regard to jurisdictional claims in published maps and institutional affiliations.